Investigation of the Influence of the Turbulent Transition on the Transonic Periodic Flow

C. Tulita[*], E. Turkbeyler[†] and S. Raghunathan[‡]

Department of Aeronautical Engineering, The Quenn's
University of Belfast, Northern Ireland,
Belfast, BT9 5AH

c.tulita@qub.ac.uk

Abstract

The effect of the turbulent transition on the onset of the transonic buffeting over the supercritical LV2F aerofoil is numerically investigated in the paper. The in-house RANS code validation has been done on 14% and 18% thick biconvex aerofoils as well as on the NACA0012 aerofoil. The importance in the results accuracy of both turbulence modelling and shock capturing approach employed is pointed out. The numerical results are compared with the most accurate CFD studies accomplished in the field of the transonic periodic flow. The RANS turbulent methodology appears to be particularly well adapted for transonic buffeting investigation where the flows strongly depend on the turbulence structure in the relatively thin boundary layer leading up to separation. The effect of the turbulent transition on buffeting onset and development can be understood as a flow control technique leading in particular conditions to complete alleviation of shock oscillations. This possible flow control technique is compared with Bump and Cavity flow control techniques, which have been applied to the same supercritical aerofoil.

Keywords: *Flow control, Buffet alleviation, CFD, RANS/LES*

Introduction

The transonic buffeting is the structural response to unsteady excitation produced by the shock-induced oscillation (SIO) triggered by the flow separation behind the shock wave. This aerodynamic phenomenon, which is related to vortex formation and structural fatigue failure, appears in many aeronautical applications such as external flow over aircraft wings as well as in internal flow around turbo-machinery blades and in compressor passages. The assessment of buffet onset associated with the proper computation of unsteady shock/boundary-layer interaction around aerofoils remains an outstanding problem in aerodynamics due to the complex physics involved. The accuracy of the SIO numerical predictions depends on both the turbulence model and the temporal and spatial accuracy of the shock capturing numerical discretisation scheme used in investigation.

The presence of a relatively strong shockwave in transonic flow has a significant influence on the development of the turbulence field in the region of the shock and on the mean flow properties upstream and downstream of the shock discontinuity. The standard turbulence models require special modifications to handle the high-pressure gradients in a physically realistic way. To that end, many models have been developed to provide accurate solutions to these flows. Generally there are three major types of turbulence methodologies which have been applied in SIO study: the Reynolds Averaged Navier Stokes RANS, the Direct Numerical Simulation (DNS) and the Large Eddy Simulation (LES) approaches.

*Research Fellow, Aeronautical Engineering
†Research Fellow, Aeronautical Engineering
‡Head, Aeronautical Engineering

Among these turbulence methodologies the RANS approach, which rely on approximate algebraic and one or two equations turbulence models, has been largely used in numerical assessments of periodic motion on biconvex, Naca0012 and supercritical aerofoils. The numerical results obtained agree qualitatively well with experiments. In fact, the periodic motion associated with the SIO phenomenon is much larger than the time scales of the wall-bounded turbulence, which is taken into account in the averaging process of RANS approach.

On the other hand, DNS has been developed to handle massive separated flows that rapidly develop strong instabilities associated with large scale structures, which overwhelms the turbulence inherited from upstream boundary layers. Hence, DNS approach attempts to solve all time and spatial scales very accurate, using extremely small grids. Both approaches have their own advantages and drawbacks. A compromise between RANS and DNS approaches, tries to model the smaller scales, like RANS, while directly solving large spatial scales like DNS. Several hybrid RANS/DNS methods have been proposed and LES is simply one of these methods.

In spite of good ability of LES to model flows which are dominated by large scale periodic features, this hybrid RANS/DNS type approach has not lead to good results in SIO investigation on aerofoils yet. A major challenge of SIO flows is their strongly dependence on the turbulence structure in the relatively thin boundary layer leading up to the separation point.

The SIO were experimentally detected over fifty years ago, but the first numerical investigation of these phenomena starts thirty years later in 1977, when Levy [1] used successfully a MacCormack's explicit scheme, with an algebraic eddy viscosity turbulence model, to the study of SIO on 18% thick biconvex aerofoil. It was concluded that turbulence models using experimental data from steady flow measurements can improve the characteristics of the periodic solutions. Since then many RANS turbulence methodologies were proposed in conjunction with implicit or explicit Navier-Stokes schemes or interactive boundary layer coupling methods, leading to improvement in the reduce frequency and, for supercritical aerofoils, in the shock wave location during the periodic motion. However, these results are obtained for the condition of full turbulent flow or when the turbulent transition is fixed at a certain location on the suction surface. The effect of the turbulent transition on the periodic motion is not fully understood even though its crucial importance on the total or partial alleviation of SIO was reported by several authors.

The paper numerically investigates the effect of the turbulent transition on SIO over a supercritical aerofoil using an implicit two-dimensional compressible Reynolds-Averaged Thin-Layer Navier-Stokes flow solver for structured grids. The spatial discretization involves a cell-centered finite-volume approach. Upwind-biasing is used for the convective and pressure terms, while central differencing is used for shear stress and heat transfer terms. The generalised Riemann problem at each cell-interface location is approximated by a collisionless Boltzmann equation and solved with van Leer's flux splitting method. Time advancement is second order accurate implicit and it is achieved with MacCormack predictor/corrector method in conjunction with Gauss-Seidel line relaxation method. The treatment of turbulence is made by a modified version of the Baldwin-Lomax turbulence model. To attenuate the numerical oscillations in the vicinity of shock waves a continuous differentiable flux limiter proposed by Mulder is used.

SIO Code Validation

Some of the principal challenges, both past and present, in CFD investigation of the transonic SIO on an aerofoil are

1. To identify a well-defined region of Mach and incidence angle where buffet occurs, taking into account possible hysteresis effects in the buffet boundaries;
2. To capture the correct Tijdeman's types of SIO on the aerofoil;
3. To capture the correct location of the oscillatory region on the aerofoil;
4. To obtain the correct reduced frequency ($k = 2\pi fc/U_\infty$) on the aerofoil.

To date there is no one CFD code, including those to be described herein, that satisfies all of the above items.

The present CFD techniques propose two major strategies to study numerically the unsteady self-sustained shock oscillations. The first consist in solving the Navier-Stokes equations directly using an implicit or explicit numeric scheme in conjunction with algebraic or non-linear turbulent models or more recently using Large Eddy Simulation. The second strategy is known as the interactive boundary layer coupling method and involves the solution of an outer inviscid region and an inner viscous boundary layer, which are coupled through the

boundary condition on the wing and wake. The effect of the turbulent viscous boundary layer is modelled in the quasi-steady manner by solving a set of ordinary differential equations in x for the integral boundary layer quantities. For enhancing the time accuracy in SIO capturing both strategies employ subiterative techniques in the context of a multigrid methodology.

18% Thick Biconvex Aerofoil Results

As an example related to the first strategy, Rumsey et al. [2] computed the periodic flow over an 18% thick biconvex aerofoil at mach numbers between M=0.72 to 0.76 and R=11 million employing implicit and explicit Navier-Stokes codes in conjunction with Roe's flux-difference-splitting shock-capturing scheme whereas all viscous terms were centrally differenced. The experimental hysteresis effect has been numerically tested under the effects of grid size, grid extent and time step in conjunction with several sub-iteration types.
Following earlier works [3] [4], which showed the importance of sub-iterations in enhancing the time accuracy of conventional implicit schemes or within the context of a multigrid methodology to allow practical time steps with the use of an explicit code, he used a five-stage Runge-Kutta time marching scheme. For turbulence modelling, both the Baldwin-Lomax [5] and the Spalart-Allmaras [6] models are employed. For M=0.76 and using the Spalart-Allmaras model he found the reduced frequency based on semi-chord values ranging from 0.46 to 0.5. These values are close to the experimental value of 0.49. On the other hand when the Baldwin-Lomax turbulence model is used, a reduced frequency of 0.37 is found. However Raghunathan et al [7] using the Baldwin-Lomax turbulence model in conjunction with an upwind van Leer implicit predictor/corrector cell-centred finite volume scheme found a reduce frequency of 0.44 over an 18% thick biconvex aerofoil where both types C and A SIO are clearly detected.

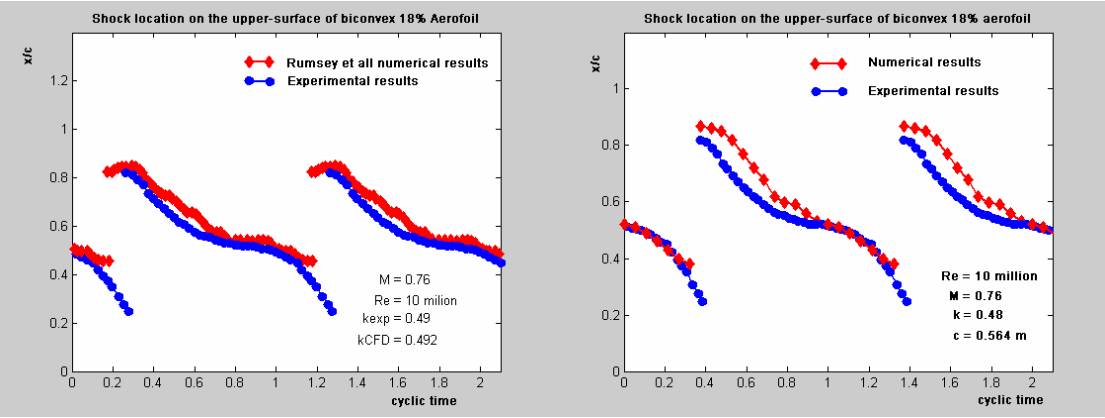

a **b**

Figure 1: Shock location on the upper-surface of an 18% thick biconvex aerofoil. a) Rumsey et al numerical results, b) Present results (M=0.76, Re=10×10^6, $\alpha=0°$, k=0.48).

As expected, and already mentioned by Deiwert, Levy [8] and Steager [9], the way of treatment of the turbulence is important for modelling separated flow and particularly SIO. However, from the previous results it can be inferred that not only the turbulence modelling is important but also the coupling between the turbulence modelling and the shock capturing approach used as well as the mesh and the turbulent transition. Rumsey employed the Baldwin-Lomax turbulence model in conjunction with Roe's shock capturing scheme whereas Raghunathan used van Leer flux-vector splitting approach. This can be explained by the different dissipative mechanism used in the FVS and FDS schemes. The form of the numerical dissipation in the FVS schemes is consistent with the Navier-Stokes viscous terms, whereas the numerical dissipation in the FDS schemes is basically inconsistent with the Navier-Stokes viscous terms, leading to the numerical shock instability and the so-called odd-even decoupling [10], which could generate spurious solutions.
As the Raghunathan's code the present in-house RANS code employs a modified version of the Baldwin-Lomax turbulence model in conjunction with an upwind van Leer implicit predictor/corrector cell-centred finite volume scheme. The reduced frequency, based on semi-chord, is 0.48 and the location of the oscillatory region on the aerofoil is comparable with that found by Rumsey (fig. 1). This improvement with respect to Raghunathan results can be explained by the second order accurate time advancement implicit scheme employment in conjunction with two sub-iterative steps in MacCormack predictor/corrector algorithm.
Figure 2 shows two last instants before the end of the type C SIO range on the upper-surface of the 18% thick

biconvex aerofoil. From figure 2 it can be inferred that the shock wave disappears upstream 40% chord. This example shows that the location of the oscillatory region on the aerofoil is not correct predicted by the both CFD codes, and this in spite of the Sparlat-Allmaras turbulence model employed by Rumsey et al.(fig. 1 a).

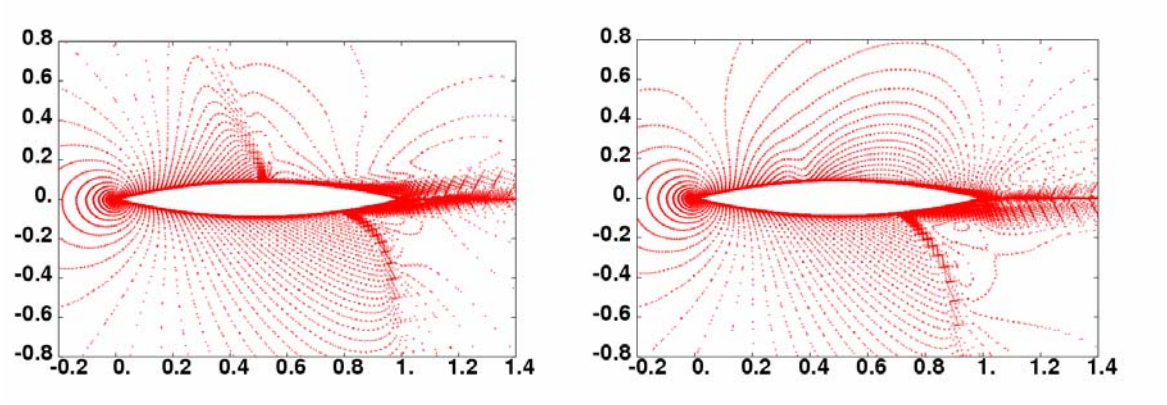

Figure 2: The end of the Type C SIO range on the upper-surface of the 18% thick biconvex aerofoil (M=0.76, $Re=10\times10^6$, $\alpha=0°$, k=0.48).

14% Thick Biconvex Aerofoil Results

For a 14% thick biconvex aerofoil the present code leads to numerical results comparing well the experimental investigations accomplished by Mabey et al. [11] at M=0.85, Reynolds 7 million and zero degrees incidence with transition fixed at x/c=0.02, where a Tijdeman's Type B SIO was experimentally detected. The computing has been accomplished at M=0.83, Reynolds 9 million and zero degrees incidence with transitin fixed at 3% chord. The experimental and computed locations of the oscillatory regions on the aerofoil are depicted into figure 3. During a part of the oscillation cycle on upper or lower aerofoil surface, the shock wave intensity decreases considerably and the shock wave almost disappears (Fig. 4, frame b and c) on the aerofoil surface. The calculated reduced frequency based on semi-chord is about 0.47 while the experimental one is approximately 0.5.

As in the cases of types A and C SIO detected on an 18% thick biconvex aerofoil, the phase difference between type B shock oscillations on upper and lower surfaces will change the effective geometry, deflecting the wake upper and lower respectively, similar to rapid deflections of a trailing edge flap. For the same aerofoil, at the upper extremity of the periodic motion domain, at M=0.86, $\alpha=0.3$, a Tijdeman's Type A SIO is identified on the aerofoil.

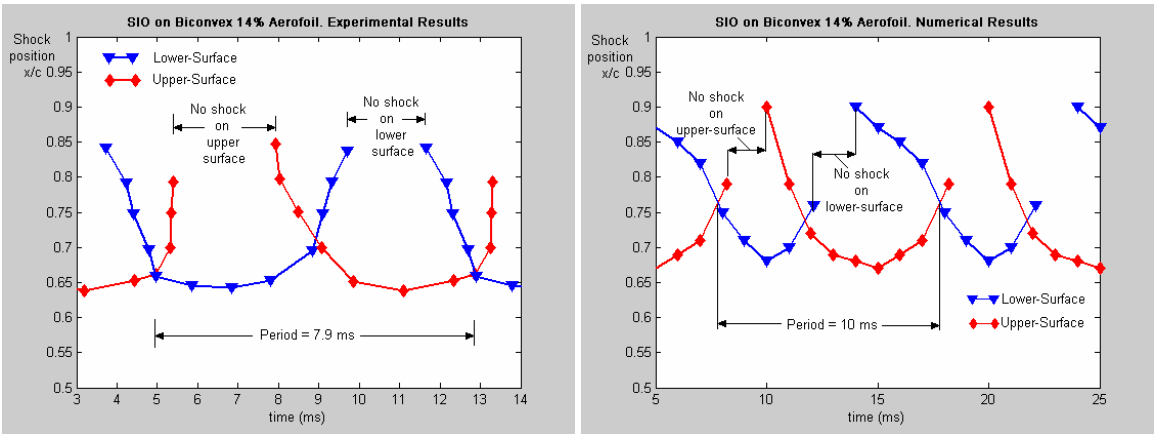

Figure 3: Shock location on the upper-surface of a 14% thick biconvex aerofoil: a) Mabey et al. experimental results (M=0.85, $Re=7\times10^6$, $\alpha=0°$, k=0.5), b) Present results (M=0.83, $Re=9\times10^6$, $\alpha=0°$, k=0.47).

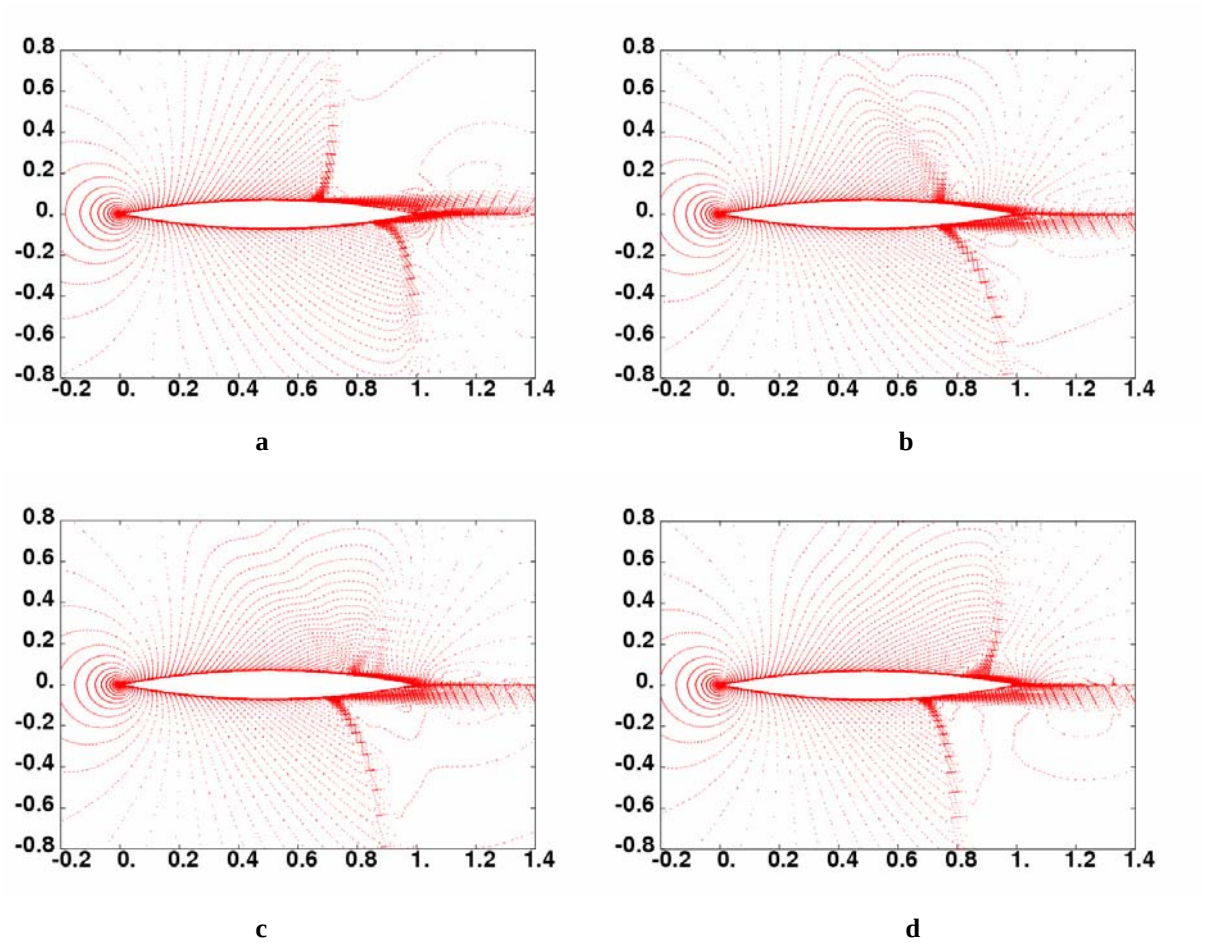

Figure 4: The disappearance of the Type B SIO on the upper-surface of the 14% thick biconvex aerofoil (frames b and c) at M=0.83, Re=9×10^6, α=0°, k=0.47.

NACA0012 Aerofoil Results

An alternative to solving RANS equations directly is the interactive boundary layer method. Among numerous viscous-inviscid interaction approaches proposed [12] [13], the method employed by Edwards [14] seems to better assess the SIO on aerofoil. In Edwards' method the coupling between the inner viscous boundary layer solution and the solution of the outer inviscid region is accomplished through the boundary conditions on the airfoil and wake.

The potential code CAP-TSD employed contains modifications developed by Batina [15] to approximate the effects of shock generated entropy and vorticity. From the leading edge of the airfoil, the boundary layer is approximated by the turbulent boundary layer on a flat plate. This assumption is suitable for attached flow boundary layer, where the effect of the turbulent viscous boundary layer is modelled in the quasi-steady manner of Green et al. [16]. When flow separation occur a velocity profile proposed by Melnik and Brook [17] is employed into an inverse boundary layer approach.

The coupling between the inverse boundary layer and the inviscid solution is accomplished using Carter's method [18], calculating the displacement thickness in conjunction with a set of coupling ordinary differential equations in time at each chord-wise location. Calculation of the boundary layer equations in the wake use an exponentially decaying wake shape modelling the upper and lower wake surfaces.

Edwards employed this algorithm to compute the buffet onset boundary and the main characteristics of periodic motion at different turbulent regimes for the 18% thick biconvex aerofoil and NACA0012 aerofoil [14].

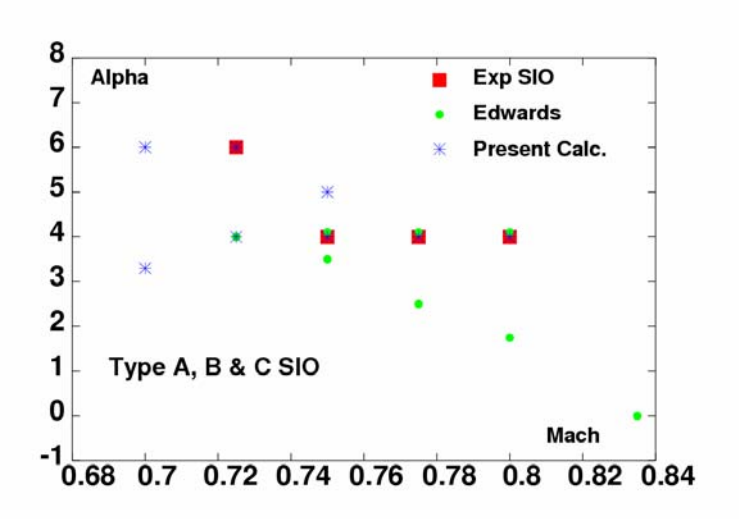

Figure 5: Transonic periodic flow over a NACA0012 aerofoil.

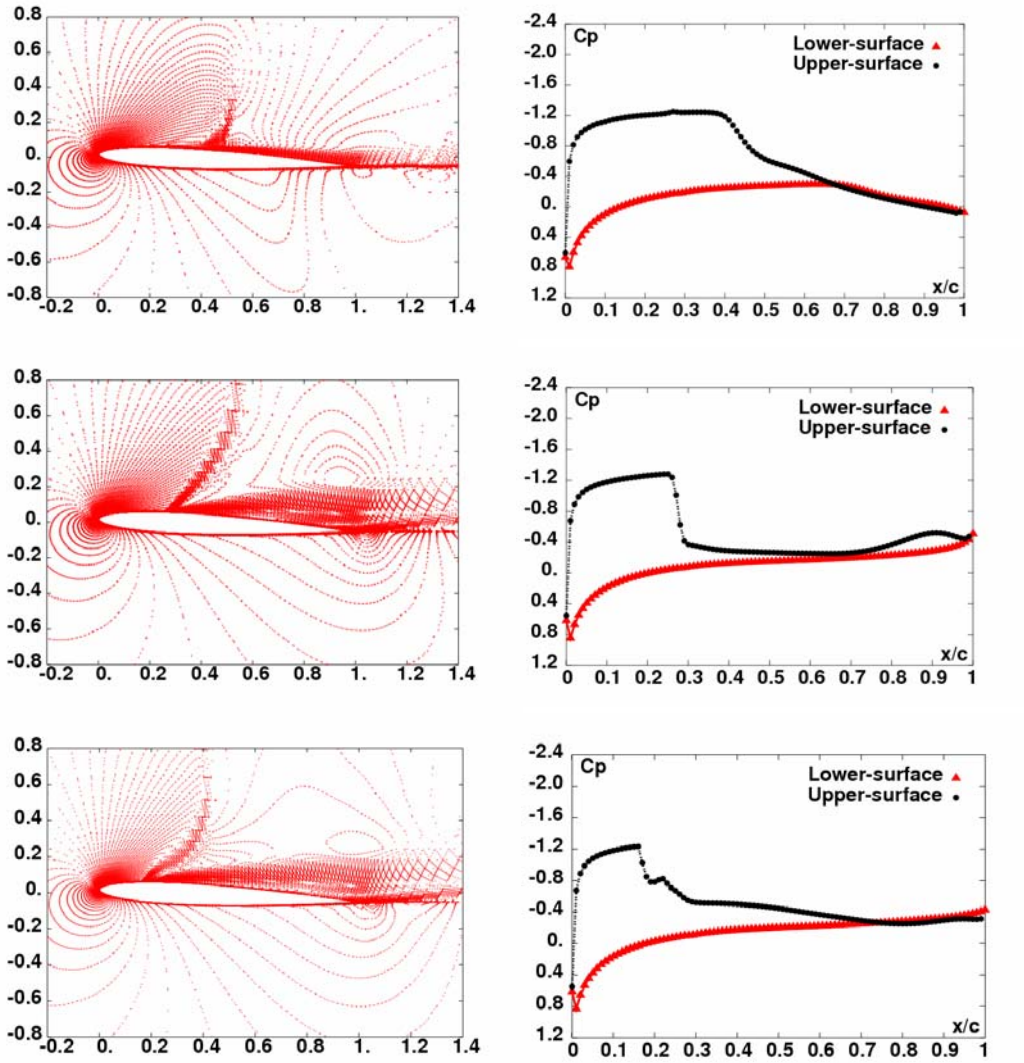

Figure 6: The type C SIO on NACA0012 aerofoil: Contours of Mach number and pressure distribution ($M=0.775$, $Re=10\times10^6$, $\alpha=4°$, $k=0.233$).

The numerical investigation show that the interactive boundary layer coupling methods lead to results that are comparable with those obtained by the most expensive Navier-Stokes codes using the RANS/LES/DNS turbulence methodologies.

In the case of the NACA0012 aerofoil, all three kinds of SIO were identified on the upper surface of the aerofoil, between 0.7 and 0.8 Mach numbers and different angles of incidence, at different Reynolds numbers based on chord, ranged from 1 to 14 million. The buffeting onset is shown to occur along a well defined boundary of mach numbers vs. angle of incidence. While the reduced frequencies range from 0.19 to 0.275, the maximum amplitude of the shock excursion is approximately 30 % chord.

The same results have been obtained with the present RANS code as illustrated into figure 5. For example at 0.775 Mach number, 10 million Reynolds number and four degrees incidence a type C SIO is detected on the suction surface of the aerofoil. The reduced frequency based on semi-chord is k=0.233 compared with 0.22 found by Edwards. The shock moves from 40% to 15% chord (fig. 6).

The influence of the turbulent transition on periodic motion

The present in-house RANS code is employed in study of the effect of the turbulence transition on the transonic periodic flow on supercritical LV2F aerofoil at T=283K, M=0.74 and four degrees incidence.
Figure 7 **a,** illustrates the experimental SIO on the LV2F aerofoil. It can be inferred the coexistence of type A and B SIO as well as the tendency of periodic motion to disappear over the aerofoil. In fact, the SIO emit pressure waves that will continually change the turbulence pattern upstream the range of the shock wave oscillation. In these conditions, there is a turbulent pattern that can be associated with the periodic motion alleviation. This can be seen between 0.866 and 0.89 seconds.

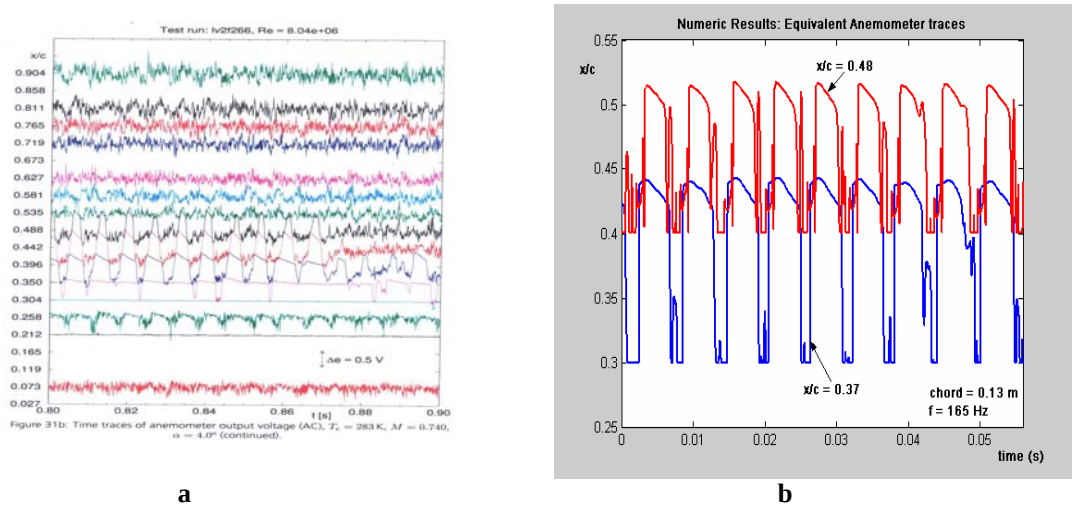

a **b**

Figure 7: Experimental and numerical anemometer traces on LV2F aerofoil (M=0.74, Re=10×10^6, α=4°, k=0.54).

On the other hand the numerical investigation can capture only one type of SIO corresponding to a certain turbulent transition point. Figure 7 **b,** illustrates the equivalent anemometer traces obtained by CFD investigation when the turbulent transition has been fixed at 32% chord and a type B SIO has been numerically captured. The experimental data have been obtained by the surface mounted cryo hot-films. These devices are often used in conventional wind tunnels and free-fight tests to measure wall shear stress and determine transition location on the model or the flight test vehicle. Since the anemometer traces from fig. 7 **a** are based on the velocity information (wall shear stress measure), the numerical results from fig. 7 **b** are also based on pressure inverse variation. The shape of the numerical traces agrees well with the experimental data.

Figure 8 shows the aerodynamic characteristic of periodic motion at 32% chord turbulent transition fixed. Figure 9 depicts Mach number field around LV2F aerofoil at different time instants during the type B SIO development. The reduced frequency based on chord is of 0.54 compared with 0.48 found experimentally. The

numerical location of the oscillatory region on the aerofoil has been found between 28% and 58% chord whereas the experimental location is between 32% and 55% chord.

From numerical investigation it was noticed that the type of SIO can be changed by modifying the turbulent transition point (Fig.10), and sometimes even completely alleviated (Fig.11). When the turbulent transition has been fixed at 7% chord a type A SIO has been identified on the aerofoil (Fig. 10). The reduced frequency is 0.49 compared with 0.48 found experimentally. On the other hand the location of the oscillatory region on the aerofoil is pulled upstream, between 20% and 50% chord, compared with the range oscillation found for 32% turbulent transition fixed.

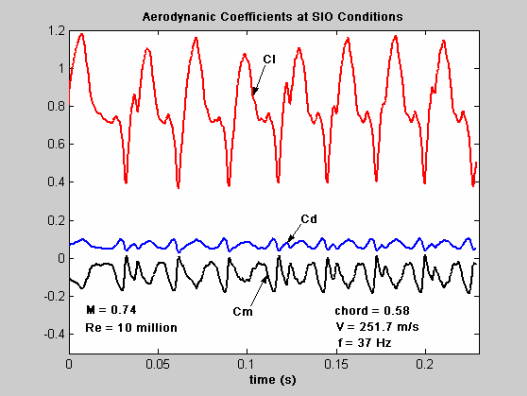

Figure 8: Type B SIO on LV2F aerofoil: Lift, drag and moment.

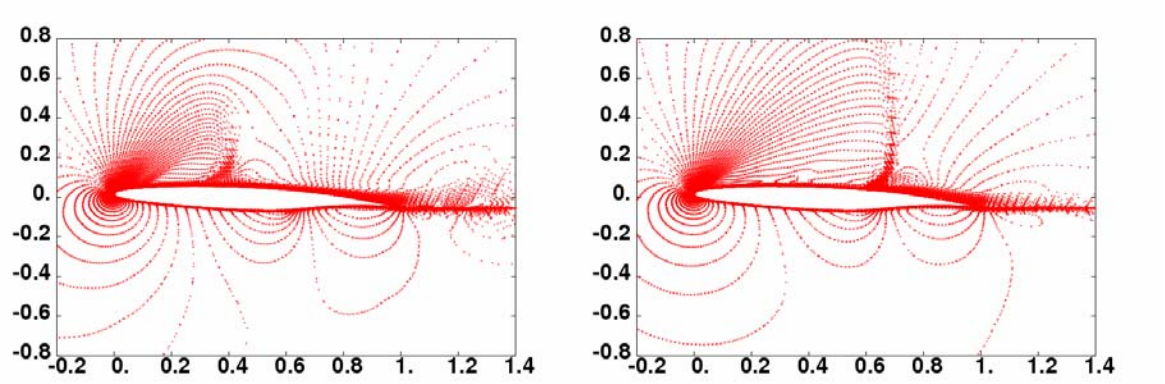

Onset of the Type B SIO

The shock downstream position

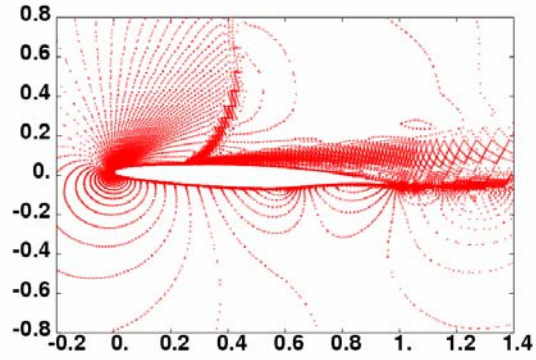

The shock upstream position

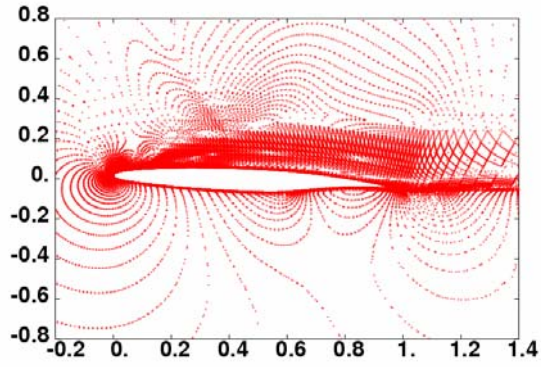

Flow without shock

Figure 9: Type B SIO on LV2F aerofoil (M=0.74, Re=10×10^6, α=4°, k=0.54).

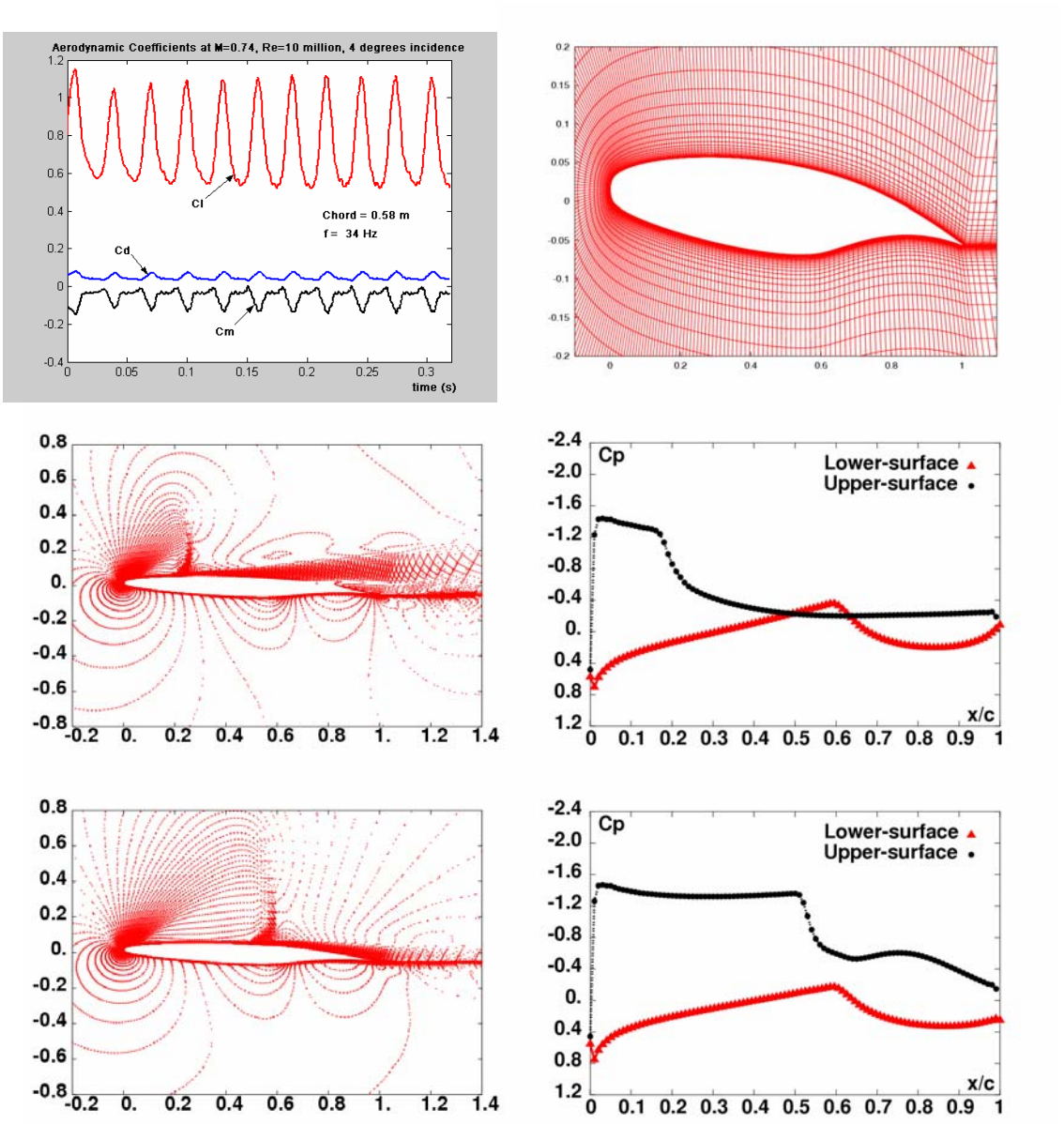

Figure 10: Type A SIO on LV2F aerofoil. Turbulent transition fixed at 7% chord.

Eventually there is a turbulent transition point (18% chord) for which the numerical results show an important buffeting alleviation (fig. 11). The effect of the turbulence onset just upstream the SIO location can be compared with a Vortex Generators actuator located in the same position. Like the Vortex Generator device, the turbulent transition gives energy to the boundary layer to stabilize the shock wave, decreasing the flow separation and implicitly alleviating buffet.

This result can also be compared with the effect of other flow control techniques on buffeting alleviation. Figure 12 illustrates the effect of a contoured bump on the periodic flow over the adaptive supercritical aerofoil (fig. 12 b). The bump, which has been located underneath the mean shock position, diminishes favorably both friction and wave drag losses by spreading the shock system, without destabilizing the boundary layer too much, while also significantly alleviating buffeting.

An equivalent effect on drag reduction and buffeting alleviation can be accomplished by using the Cavity Flow Control technique (fig. 13). As in the case of the Bump Flow Control technique, the cavity has been located underneath the mean shock position as it can be seen from figure 13 b. The Bump and Cavity techniques obviously lead to buffet alleviation. On the other hand, the Cavity technique seems to be more effective at increasing the lift-to-drag ration than the Bump technique. However, their effect on the drag in periodic flow is still unclear and requires further investigation.

From the numerical results presented can be inferred that both Cavity and Bump techniques lead to a better aerodynamic ration between lift and drag than the result obtained with the turbulent transition fixed at 18% chord (fig. 11). However all these concept are very effective at alleviating buffeting.
From the numerical results presented can be inferred that both Cavity and Bump techniques lead to a better aerodynamic ration between lift and drag than the result obtained with the turbulent transition fixed at 18% chord (fig. 11). However all these concept are very effective at alleviating buffeting.

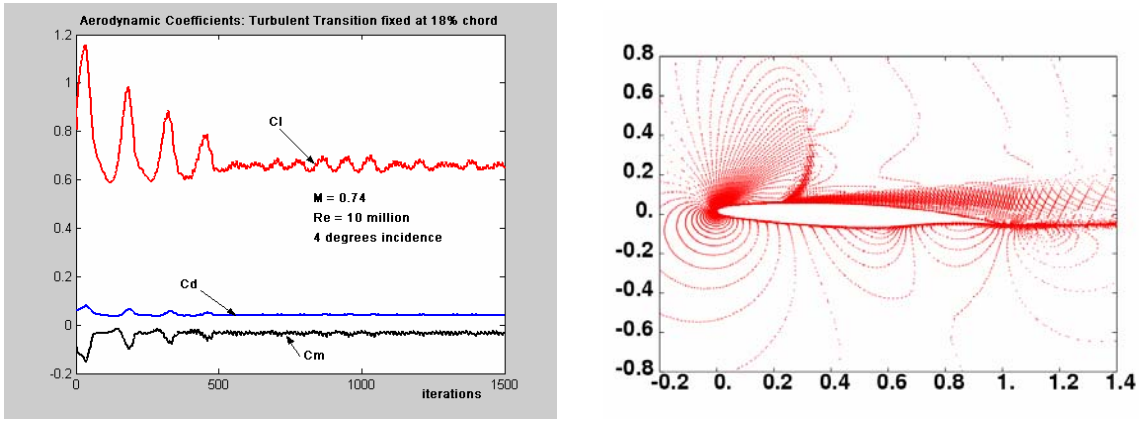

Figure 11: Buffeting alleviation. Turbulent transition fixed at 18% chord.

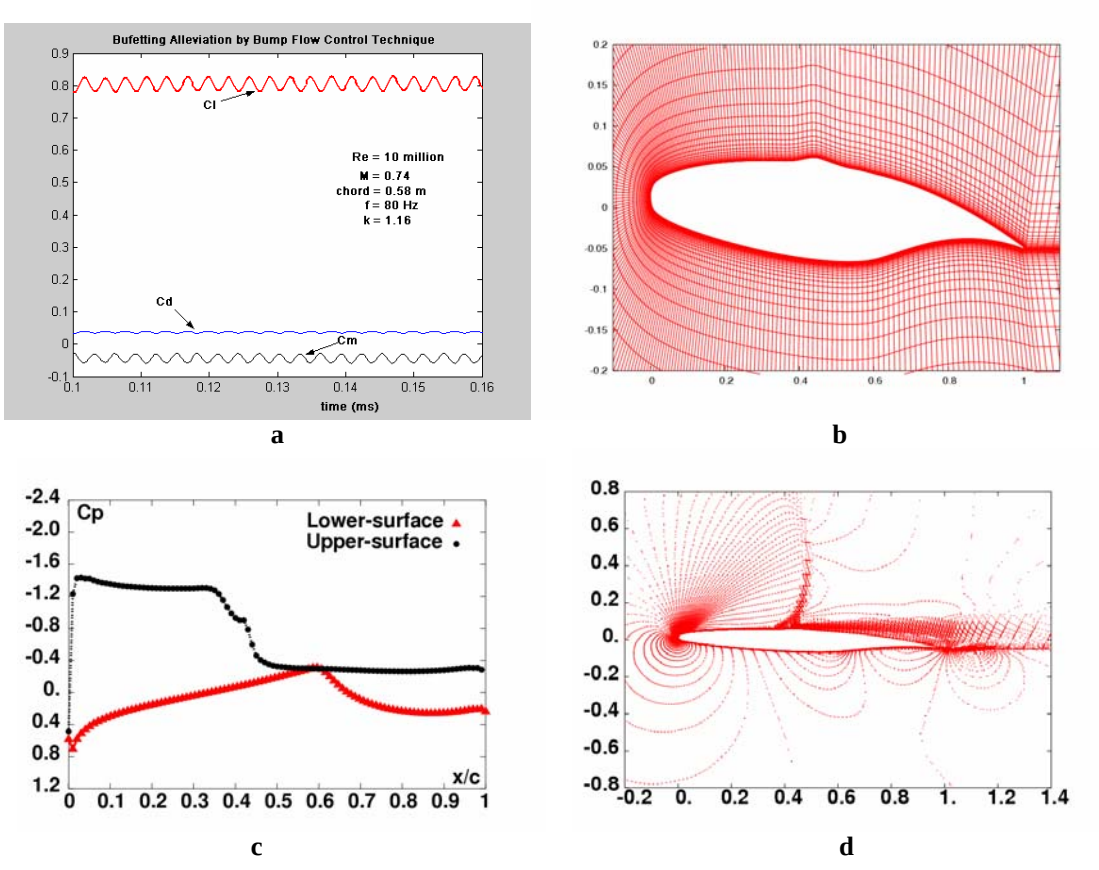

Figure 12: Buffeting alleviation by Contour Bump technique (M=0.74, Re=10×10^6, α=4°).

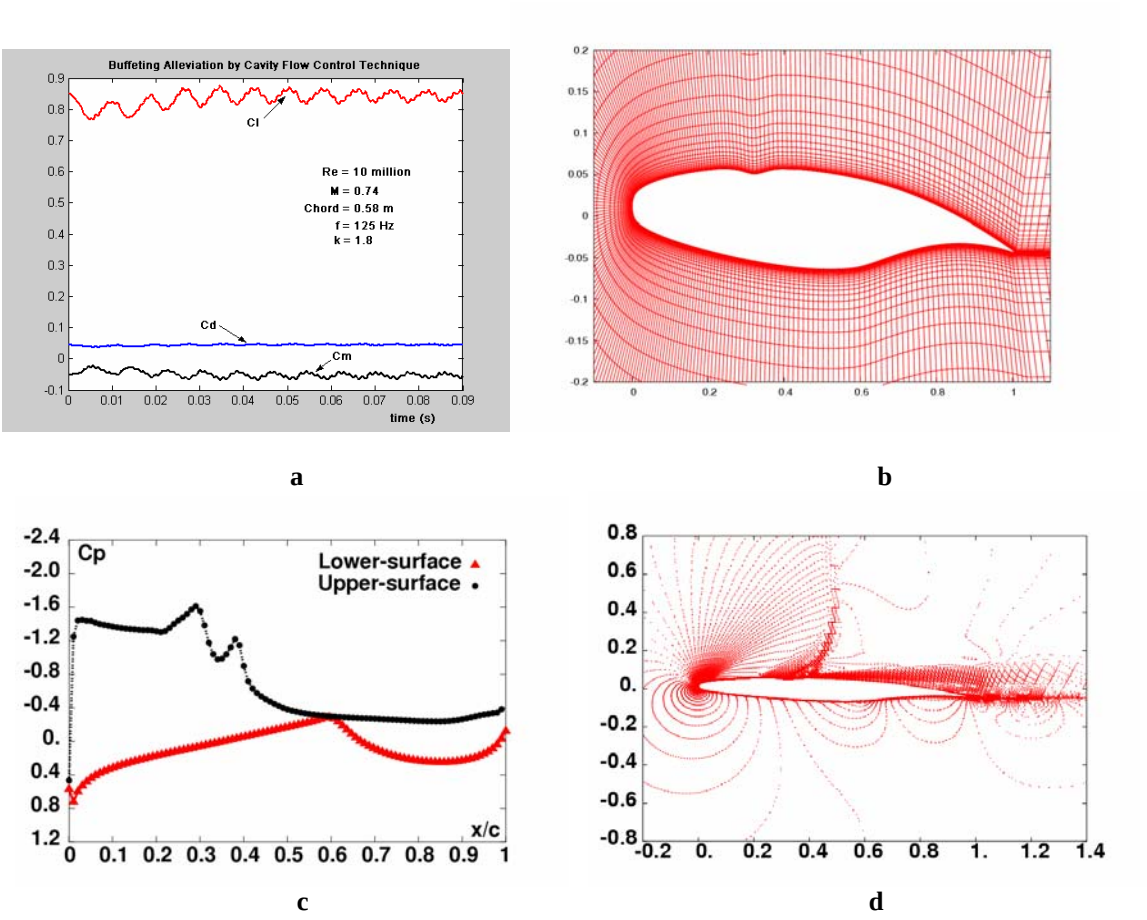

Figure 13: Buffeting alleviation by Cavity technique (M=0.74, Re=10×10^6, α=4°).

Conclusion

CFD investigation has been carried on in order to understand the effect of the turbulent transition on buffeting onset and development. An in-house RANS code has been employed in conjunction with a modified Boldwin-Lomax turbulence model. The code was validated in the usual CFD limits related to SIO on biconvex and NACA0012 aerofoils. From the numerical results can be inferred the crucial importance the turbulent transition has on transonic buffeting around an aerofoil. The variation of the transition point on the aerofoil can change the type and the characteristics of the periodic flow, even leading to the strong alleviation of buffeting.

References

1. L L Levy Jr. Experimental and computational steady unsteady transonic flows about a thick airfoil. AIAA Journal, Vol. 16, pp. 564-572, 1978.
2. CL Rumsey, MD Sanetrik, RT Biedron, ND Melson, EB Parlette. Efficiency and accuracy of time-accurate turbulent Navier-Stokes computations. AIAA paper 95-1835.
3. T. Pulliam. Time accuracy and the Use of Implicit Methods, AIAA paper 93-3360-CP, July 1993.
4. A. Jameson. Time Dependent Calculations Using Multigrid, with Applications to Unsteady Flows Past Airfoils and Wings, AIAA paper 91-1596.
5. B Baldwin, H. Lomax. Thin Layer Approximation and Algebraic Model for Separated Turbulent Flow. AIAA paper 78-257.
6. P. Spalart and S. Allmaras. A one Equation Turbulence Model for Aerodynamic Flows, AIAA paper 92-0439.

7. S. Raghunathan, MA Gillan, RK Cooper, RD Mitchell, JS Cole. Shock oscillations on biconvex aerofoils. Aerosp Sci Technol 1999; 3(1):1-9.
8. GS Deiwert. Numerical Simulation of High Reynolds Number Transonic Flows. AIAA Journal, Vol. 13, pp. 1354-1359, 1975.
9. JL Steger. Implicit finite-difference simulation of flow about arbitrary two-dimensional geometries. AIAA Journal, Vol.16, p.679-686, 1978.
10. JJ Quirk. A contribution to the great Riemann solver debate. International Journal for Numerical Methods in Fluids. Vol. 18, 555-574, 1994.
11. DG Mabey, BL Welsh, BE Cripps. Periodic flows on a rigid 14% thick biconvex wing at transonic speeds. TR 81059, Royal Aircraft Etablishmant, May 1981.
12. JC Le Balleur. Computation of flows including viscous interactions with coupling methods. General Introduction Lecture 1, AGARD CP-291, computation of viscous-inviscid interactions, United States Air Force Academy. Colorado Springs Colorado, USA, 29 Sept.-1 Oct. 1980.
13. P. Girodroux-Lavigne, JC Le Balleur. Time-consistent computation of transonic buffet over airfoils. Proceedings of 16th Congress of the International Council of the Aeronautical Sciences, ICAS 88-5.52, 1988. p.779-87.
14. JW Edwards. Transonic shock oscillations calculated with a new interactive boundary layer coupling method. AIAA 93-0777, 31st Aerospace Sciences Meeting and Exhibit, Reno, Nevada, January 1993.
15. JT Batina. Unsteady Transonic Small-Disturbance Theory Including Entropy and Vorticity Effects. Journal of Aircraft, Vol. 26, June 1989, p. 531-538.
16. JE Green, DJ Weeks, JWF Brooman. Prediction of Turbulent Boundary Layers and Wakes in Compressible Flow by a Lag- Entrainment Method. R&M No. 3791, British Aeronautical research Council, 1977.
17. RE Melnik, JW Brook. The Computation of Viscid/Inviscid Interaction on Airfoils With Separated Flow. Third Symposium on Numerical and Physical aspects of Aerodinamic Flows, California State University, 1985, p. 1-21-1-37.
18. JE Carter. A new boundary-layer inviscid interaction technique for separated flows. AIAA paper 79-1450.